Aalto University

Aaltodoc
OPEN ACCESS

This is an electronic reprint of the original article.
This reprint may differ from the original in pagination and typographic detail.

Author(s): Repo, Päivikki & Benick, Jan & Gastrow, Guillaume von & Vähänissi, Ville & Heinz, Friedemann D. & Schön, Jonas & Schubert, Martin C. & Savin, Hele

Title: Passivation of black silicon boron emitters with atomic layer deposited aluminum oxide

Year: 2013

Version: Post print

Please cite the original version:

Repo, Päivikki & Benick, Jan & Gastrow, Guillaume von & Vähänissi, Ville & Heinz, Friedemann D. & Schön, Jonas & Schubert, Martin C. & Savin, Hele. 2013. Passivation of black silicon boron emitters with atomic layer deposited aluminum oxide. Physica Status Solidi RRL. Volume 7, Issue 11. 950-954. DOI: 10.1002/pssr.201308096.

Rights: © 2013 Wiley-Blackwell. This is the post print version of the following article: Repo, Päivikki & Benick, Jan & Gastrow, Guillaume von & Vähänissi, Ville & Heinz, Friedemann D. & Schön, Jonas & Schubert, Martin C. & Savin, Hele. 2013. Passivation of black silicon boron emitters with atomic layer deposited aluminum oxide. Physica Status Solidi RRL. Volume 7, Issue 11. 950-954. DOI: 10.1002/pssr.201308096, which has been published in final form at http://onlinelibrary.wiley.com/doi/10.1002/pssr.201308096/abstract.

All material supplied via Aaltodoc is protected by copyright and other intellectual property rights, and duplication or sale of all or part of any of the repository collections is not permitted, except that material may be duplicated by you for your research use or educational purposes in electronic or print form. You must obtain permission for any other use. Electronic or print copies may not be offered, whether for sale or otherwise to anyone who is not an authorised user.

Passivation of black silicon boron emitters with atomic layer deposited aluminum oxide

Päivikki Repo[*,1], Jan Benick[2], Guillaume von Gastrow[1], Ville Vähänissi[1], Friedemann D. Heinz[2], Jonas Schön[2], Martin C. Schubert[2], and Hele Savin[1]

[1] Department of Micro- and Nanosciences, Aalto University, Tietotie 3, 02150 Espoo, Finland
[2] Division Solar Cells - Development and Characterization, Fraunhofer Institute for Solar Energy Systems (ISE), Heidenhofstraße 2, 79110 Freiburg, Germany

Keywords black silicon, surface passivation, boron diffusion, aluminum oxide

The nanostructured surface - also called black silicon (b-Si) - is a promising texture for solar cells because of its extremely low reflectance combined with low surface recombination obtained with atomic layer deposited (ALD) thin films. However, the challenges in keeping the excellent optical properties and passivation in further processing have not been addressed before. Here we study especially the applicability of the ALD passivation on highly boron doped emitters that is present in crystalline silicon solar cells. The results show that the nanostructured boron emitters can be passivated efficiently using ALD Al_2O_3 reaching emitter saturation current densities as low as 51 fA/cm^2. (Removed: However, the nanostructures are known to cause enhanced surface recombination and are physically vulnerable for further processing. In crystalline silicon solar cells, the nanostructures need to survive several processing steps and be well passivated at the end. Emitter saturation current densities of 51 fA/cm^2 prove that the nanostructured boron emitters can be passivated efficiently using ALD Al_2O_3.) Furthermore, reflectance values less than 0.5 % after processing show that the different process steps are not detrimental for the low reflectance of b-Si.

Copyright line will be provided by the publisher

1 Introduction Black silicon (b-Si) has attracted attention in many research fields, especially in the photovoltaic and photodetector community because of its low surface reflectance of even below 1% over a large wavelength range [1, 2]. However, one major challenge has been the reduction of the increased recombination of charge carriers caused by the large area of the nanostructured surface. This causes poor spectral response especially at short-wavelengths [3]. Black silicon has been mostly applied on p-type cells using both thermal oxidation [4] and PECVD (plasma-enhanced chemical vapor deposition) SiN_x [5, 6] for the front surface passivation. Especially in the case of SiNx the poor conformality of the PECVD film has resulted in insufficient passivation [5, 6]. The highest obtained efficiency of a p-type black silicon solar cell with thermal oxide as the front surface passivation material is 18.2 % [7].

Reactive ion etching (RIE) process is a well-known method to fabricate black-silicon, although it was originally considered as an undesirable etching result and was used mainly for optimizing the etching parameters to produce vertical sidewalls [8]. Besides RIE, other methods for b-Si fabrication, such as laser texturing [9], metal-catalyzed wet chemical etching [10] or plasma immersion ion implantation [5] have been suggested. Also, the applications for b-Si besides photovoltaics and photodetectors [11] are numerous including microelectromechanical systems (MEMS) [12], ion mobility spectrometers (IMS) [13], terahertz emitters [14], and drug analysis [15]. One interesting aspect of black silicon surfaces is their superhydrophobicity which opens up the possibility to make them self-cleaning [16]. Using RIE for b-Si etching has certain advantages: it is relatively fast and inexpensive and nanostructures can be made without mask layers [2]. In addition, in an RIE the etch rate is independent of crystalline planes which is an issue in wet chemical etching.

In recent years Al_2O_3 has been considered to be one of the most promising silicon surface passivation materials [17-19]. The passivation ability of Al_2O_3 is related to the combination of low defect density and negative fixed charge at the Si/ Al_2O_3 interface. These properties make it promising for passivation of lowly doped n- and p-type as well as highly doped p-type surfaces [20, 21]. Atomic layer deposited (ALD) Al_2O_3 provides the lowest surface recombination velocities compared to Al_2O_3 deposited by other methods such as PECVD or sputtering [22] and because of its conformality [23] we consider ALD as a natural choice for the coating of nanostructured b-Si surfaces.

Copyright line will be provided by the publisher

We have previously shown that b-Si surfaces can be sufficiently passivated with ALD Al_2O_3 and that Al_2O_3 acts as an antireflection coating and reduces the already low reflectance of b-Si even below 1 % both in mono- and multicrystalline silicon [24, 25]. The next step is naturally to study the passivation of the emitters by the same method. Moreover, the other black silicon solar cell studies have mainly concentrated on entire cell structures, thereby the emitter formation and its passivation has not been systematically studied before. In this paper, therefore, we focus on two important questions: i) Is the black silicon surface passivation by ALD still efficient after emitter formation? ii) Does the dopant glass removal have an effect on the nanostructures and the reflectance? The changes in the nanostructure after different diffusion processes are investigated by reflectance measurements and scanning electron microscopy (SEM). To estimate the emitter profile both simulations and UV micro Raman Spectroscopy [26] are applied. The passivation quality of Al_2O_3 on boron doped black silicon emitters is evaluated by extracting the emitter saturation current density J_{0e} from minority carrier lifetime measurements.

2 Experimental details Black silicon was fabricated using a maskless cryogenic deep reactive ion etching process (ICP-RIE, Plasmalab System 100, Oxford Instruments) at -120 °C. Both sides of each 4 inch n-type FZ wafer (5 Ωcm, 400 µm) were etched to produce symmetric samples for emitter saturation current measurements. A mixture of SF_6/O_2 was used as the etching gas and their flows were set to 40 sccm and 18 sccm, respectively while the powers of inductively and capacitively coupled power sources were 1000 W and 2 W.

After the b-Si etching, the samples went through a standard RCA-cleaning (SC1 + SC2 + HF-dip). Two diffusion temperatures, 890 °C and 910 °C, were chosen for double-sided BBr3 tube furnace diffusion. On a planar surface, diffusion at 890 °C or at 910°C for an hour should lead to emitters with a sheet resistance of ~90 Ω/sq and ~70 Ω/sq, respectively. In addition some of the samples went through a 1h drive-in oxidation at 1050 °C after the diffusion at 890 °C in order to lower the surface doping and have a deeper emitter profile. Table 1 summarizes the three studied process sequences. The boron silicate glass (BSG) was etched off in 50 % HF (2 min) after the diffusion. In samples which had additional drive-in oxidation, the glass was removed before the oxidation (see table 1). (Removed: After the diffusion and especially before the drive-in oxidation the boron silicate glass (BSG) was etched away in 50 % HF (2 min).)

Al_2O_3 was deposited on both wafer sides with plasma-assisted ALD (PA-ALD) at 180 °C using Trimethylaluminum (TMA) as the aluminum source. The total cycle time was 7 seconds and 78 cycles led to a layer thickness of around 10 nm. The passivation was activated with a forming gas anneal (FGA) at 425 °C for 25 minutes.

Table 1 The different processing sequences implemented in this study.

Diffusion temperature & time	BSG etching	Drive-in oxidation	Passivation
890 °C, 1 h	50 % HF	-	Al_2O_3
910 °C, 1 h	50 % HF	-	Al_2O_3
890 °C, 1 h	50 % HF	1050 °C	Al_2O_3

To evaluate the passivation quality the emitter saturation current density J_{0e} of the b-Si emitters after the boron diffusion at 910 ºC and with Al_2O_3 passivation was extracted from the quasi-steady-state photoconductance measurements (QSSPC, Sinton WCT-120) by using the high injection method [27]. In this method the J_{0e} value is estimated from the slope of the linear fit to the curve of the inverse effective lifetime subtracted by the intrinsic bulk lifetime, $1/\tau_{eff}$-$1/\tau_{bulk,intr}$, as a function of the injection level Δn. Here, the fitting was done around the injection level of 1×10^{16} cm^{-3}. In the J_{0e} calculation an intrinsic carrier concentration n_i of 8.6×10^9 cm^{-3} (25 °C) and a revised Auger parametrization according to Richter et al. [28] were used. Using the one-diode equation and omitting the effect of the recombination at the rear side and in the base we can estimate a maximum open-circuit voltage $V_{oc,max}$ for the b-Si samples and eventually for a b-Si n-type solar cell:

$$V_{oc,\max} = \frac{k_B T}{q} \ln\left(\frac{J_{sc}}{J_{0e}} + 1\right) \quad (1)$$

where k_B is the Boltzmann constant, q the elementary charge, T the temperature and J_{sc} the short-circuit current density.

3 Results and discussion We evaluate the changes in the nanostructures by measuring the reflectance before and after different diffusion processes. In Fig. 1a the b-Si reflectance after the diffusion at 910 °C is compared to the measured reflectance of random pyramids coated with SiO_x/SiN_x (8 nm/65 nm) as well as inverted pyramids with an Al_2O_3/SiN_x stack (10 nm/65 nm). The AM1.5G spectrum weighted average reflectances R_w were calculated in the wavelength range 300 – 1200 nm. The escape is omitted in the R_w calculations as well as in the reflectances shown in the figures by assuming the front surface reflectance to be linear for $\lambda > 900$ nm and by extrapolating the measured reflectance. In the short wavelength range the b-Si reflectance is much lower than in the reference samples whereas in the mid-wavelength range the reference samples exhibits slightly smaller reflectance values because of the SiN_x anti-reflection coating with near zero reflectance at 600 nm. R_w is however smallest in the black silicon sample (~0.7 %) even after processing and only with 10 nm Al_2O_3 on the front surface.

In Fig. 1b the reflectance of b-Si surfaces after different diffusion processes as well as in the initial state, i.e directly after etching, is shown. Surprisingly, there are no significant

Copyright line will be provided by the publisher

changes in the reflectance even in the sample having combination of diffusion and a following drive-in oxidation. The small increase in the reflectance indicates that there can be some changes in the nanostructure. This can be verified by the SEM images in Fig. 2 where the b-Si structure is shown before and after diffusion and drive-in. Indeed, small changes in the nanostructure height and shape can be seen, i.e. the needles become shorter and sharper. The fact that diffusion can be done without causing drastic changes in the reflectance gives more freedom also in the optimization of the emitter profile i.e. if a deeper emitter is needed a drive-in can be applied without losing the good optical properties of black silicon. The small increase in the reflectance indicates that there can be some changes in the nanostructure.

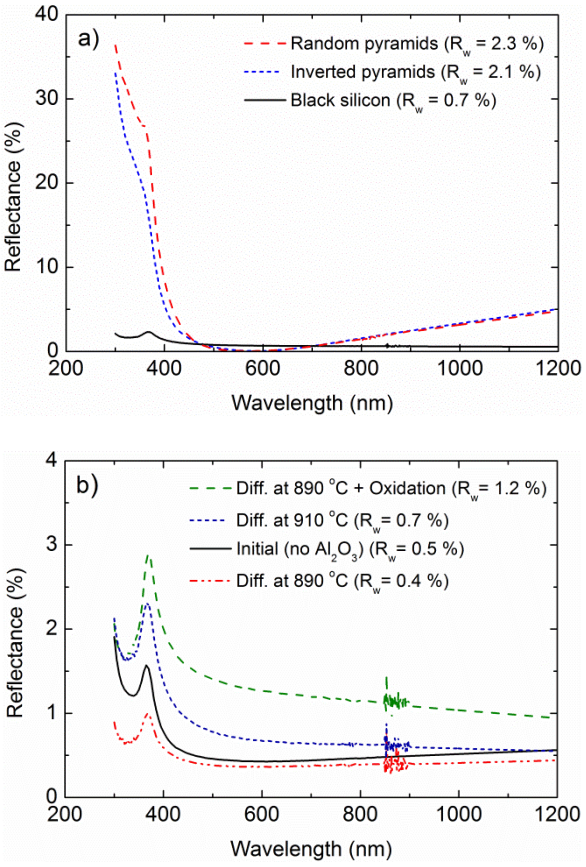

Figure 1 In a) the b-Si reflectance (after diffusion at 910 °C and Al_2O_3 deposition) and the reflectance from random and inverted pyramids are shown. For passivation and antireflection there is a SiO_2/SiN_x stack in the random pyramid sample and Al_2O_3/SiN_x stack in the inverted pyramid sample. b) presents the initial b-Si reflectance and the reflectances after different diffusion processes. Al_2O_3 was deposited on the diffused samples. The escape reflection is removed from the curves and also ignored in the calculation of the spectrum weighted average reflectances (calculated between 300 nm and 1200 nm).

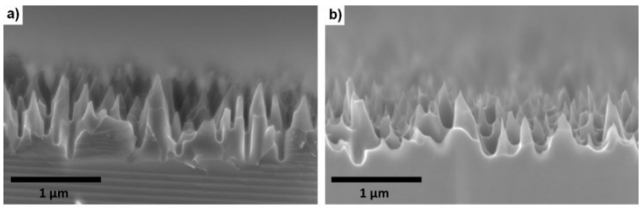

Figure 2 SEM image from a black silicon surface a) before and b) after boron diffusion at 890 °C and the subsequent drive-in oxidation. Boron glass was removed before the drive-in oxidation. With close examination small changes in the nanostructures can be seen. This is coherent with the reflectance results and is caused by the consumption of silicon during the boron glass formation and the drive-in oxidation.

Our simulations with Sentaurus Process [29] indicate that all diffusion processes used in this study lead to a complete doping of the nanostructure i.e. the junction is nearly flat under the surface and only mildly follows the surface structure. This and the final emitter profile naturally depend on the diffusion process. The consumption of silicon during the boron glass formation and the drive-in oxidation was taken into account in the simulations [30]. To investigate whether a homogeneous emitter depth inside the silicon bulk is established, two dimensional doping density measurements on polished cross section cuts using UV micro Raman Spectroscopy [26, 31] was performed. Fig. 3a shows the measured doping density of the 890°C diffused and Fig. 3b the 890°C diffused and oxidized sample within the bulk beneath the needle structure (the sample surface was estimated from the Raman scattering intensity). Both measurements are scaled identically. The doping depth (drop of doping density from the bottom of the needles to below the detection limit of $3 \cdot 10^{17}$ cm^{-3} inside the bulk) can be readily estimated to be less than 400 nm for the diffused and 1.5 µm for the oxidized sample. Furthermore it can be seen clearly that in both cases a homogeneous doping profile depth was established. On the right of the measured emitters in Fig. 3a and b the doping profiles simulated with Sentaurus Process are depicted. It can be seen that the doping concentration as well as the emitter depth is predicted well by the Sentaurus Process simulation in comparison to the micro Raman measurement. The smoother drop of the measured doping density can be well understood by a signal smearing due to measuring at the spatial resolution limit. The dashed line depicts the simulated p/n junction, which in both cases is predicted of being developed homogeneously.

Copyright line will be provided by the publisher

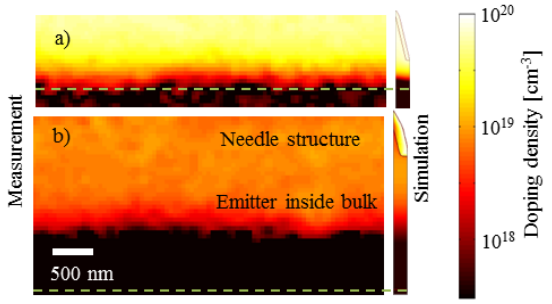

Figure 3 The measured doping density of a) the 890°C diffused and b) 890°C diffused and oxidized sample. Both measurements are scaled identically

Fig. 4 shows the measured inverse effective lifetime and the corresponding emitter saturation current J_{0e} of the most industrially relevant b-Si sample, i. e. after diffusion at 910 °C. J_{0e} value of 51 fA/cm^2 prove that an efficient surface passivation can be obtained with an industrial type of emitter. (Removed: The measured inverse effective lifetime and the corresponding emitter saturation current J_{0e} of the b-Si sample after diffusion at 910 °C is shown in Fig. 4. J_{0e} value of 51 fA/cm^2 prove that an efficient surface passivation can be obtained with this emitter.) As a reference, J_{0e} values as low as ~11 fA/cm^2 have been reached on high efficiency boron emitters and 20-25 fA/cm^2 on more industrial type emitters with Al_2O_3 passivation [32]. These results are for planar surfaces and naturally for textured surfaces the values are higher: for industrial type emitters with random pyramids J_{0e} values of ~45 fA/cm^2 are reached when using Al_2O_3/SiN_x stacks for surface passivation [33]. The $V_{oc,max}$ value of 703 mV was calculated with Eq. (1). (T = 25 °C, J_{sc} = 40 mA/cm^2) proving that black silicon with Al_2O_3 surface passivation could be applied on high-efficiency n-type solar cells. The effective lifetime τ_{eff} at an injection level of 1×10^{15} cm^{-3} is 0.78 ms and the implied open-circuit voltage $V_{oc,impl}$ = 688 mV (at 1 sun), both measured with QSSPC. If a symmetrical structure is assumed (i.e. emitters on both surfaces are taken into account in the calculation $2\times J_{0e}$ = fA/cm^2) the one-diode model gives a maximum open circuit voltage of 686 mV. This is in good agreement with the measured implied V_{oc} value.

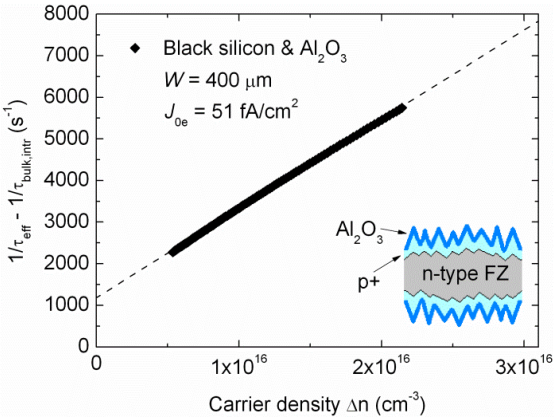

Figure 4 The inverse effective lifetime corrected with the intrinsic bulk lifetime as a function of injection level. The corresponding linear fit is shown with a dotted line and the inset presents a schematic of the J_{0e} sample.

4 Conclusions In this work we have shown that Al_2O_3 provides efficient surface passivation on nanostructured boron doped emitters, which is the first step towards high efficiency n-type black silicon solar cells. With an emitter saturation current density of 51 fA/cm^2 open-circuit voltages of around 700 mV are achievable. We have also investigated the effects of different diffusion processes on the optical properties of low-reflectivity black silicon and shown that although there is a change in the nanostructure extremely low average reflectance values – even as low as 0.5 % - can still be reached after depositing a thin layer of Al_2O_3. These results show that diffusion can be applied on a black silicon surface without losing the good optical properties and prove the potential of using black silicon as the front surface texture on a high-efficient n-type solar cells.

Acknowledgements The authors thank F. Schätzle, K. Zimmermann, J. Zielonka and S. Seitz from Faunhofer ISE for the support with processing and characterization and A. Richter for the help with the J0e evaluation. C. Reichel is thanked for providing the reference reflectance data. P. Repo acknowledges the Graduate School of the Faculty of Electronics, Communications and Automation for the financial support. Aalto University at Micronova Nanofabrication Centre is acknowledged for the provision of facilities.

References

[1] J. Li, H. Yu Yu, and Y. Li, Nanoscale **3**, 4888 (2011).
[2] L. Sainiemi, V. Jokinen, A. Shah, M. Shpak, S. Aura, P. Su-vanto, and S. Franssila, Adv. Mater. **23**, 122 (2011).
[3] H.-C. Yuan, V. E. Yost, M. R. Page, P. Stradins, D. L. Meier, and H. M. Branz, Appl. Phys. Lett. **95**, 123501 (2009).
[4] S. Koynov, M. S. Brandt, and M. Stutzmann , Phys. Stat. Sol. RRL **1**, R53 (2007).
[5] Y. Xia, B. Liu, J. Liu, Z. Shen, and C. Li, Sol. Energy **85**, 1574 (2011).
[6] D. Z. Dimitrov and C.-H. Du, Appl. Surf. Sci., Accepted for publication (2012).
[7] J J. Oh, H.-C. Yuan, and H. M. Branz, Nature Nanotechnology **7**, 743 (2012).
[8] H. Jansen, M. de Boer, R. Legtenberg, and M. Elwenspoek, J. Micromech. Microeng. **5**, 115 (1995).
[9] M. Halbwax, T. Sarnet, Ph. Delaporte, M. Sentis, H. Etienne, F. Torregrosa, V. Vervisch, I. Perichaud, and S. Martinuzzi, Thin Solid Films **516**, 6791 (2008).
[10] S. Koynov, M. S. Brandt, and M. Stutzmann, Appl. Phys. Lett. **88**, 203107 (2006).
[11] J. Z. Huang, J. E. Carey, M. Liu, X. Guo, E. Mazur, and J. C. Campbell, Appl. Phys. Lett. **89**, 033506 (2006).
[12] M. J. de Boer, J. G. E. (H.) Gardeniers, H. V. Jansen, E. Smulders, M.-J. Gilde, G. Roelofs, J. N. Sasserath, and M. Elwenspoek, J. Micromech. Microeng. **11**, 385 (2002).

Copyright line will be provided by the publisher

[13] B. Gesemann, R. Wehrspohn, A. Hackner, and G. Müller, IEEE Trans. Nanotechnol. **10**, 50 (2011).
[14] P. Hoyer, M. Theuer, R. Beigang, and E.-B. Kley, Appl. Phys. Lett. **93**, 091106 (2008).
[15] L. Sainiemi, H. Keskinen, M. Aromaa, L. Luosujärvi, K. Grigoras, T. Kotiaho, J. M. Mäkelä, and S. Franssila, Nanotechnology **18**, 505303 (2007).
[16] J. Zhu, C.-M. Hsu, Z. Yu, S. Fan, and Y. Cui, Nanolett. **10**, 1979 (2010).
[17] B. Hoex, J. Schmidt, P. Pohl, M. C. M. van de Sanden, and W. M. M. Kessels, J. Appl. Phys. **104**, 044903 (2008).
[18] G. Dingemans, R. Seguin, P. Engelhart, M. C. M. van de Sanden, and W. M. M. Kessels, Phys. Stat. Sol. RRL **4**, 10 (2010).
[19] J. Schmidt, B. Veith, and R. Brendel, Phys. Stat. Sol. RRL **3**, 287 (2009).
[20] J. Benick, B. Hoex, M. C. M.van de Sanden, W. M. M. Kes-sels, O. Schultz, and S. W. Glunz, Appl. Phys. Lett. **92**, 253504 (2008).
[21] M. A. Green, K. Emery, Y. Hishikawa, and W. Warta, Prog. Photovolt.: Res. Appl. **18**, 144 (2010).
[22] J. Schmidt, F. Werner, B. Veith, D. Zielke, R. Bock, R. Brendel, V. Tiba, P. Poodt, F. Roozeboom. A. Li, and A. Cuevas, Photovoltaics International, **10**, 42 (2010).
[23] J. L. van Hemmen, S. B. S. Heil, J. H. Klootwijk, F. Roozeboom, C. J. Hodson, M. C. M.van de Sanden, and W. M. M. Kessels, J. Elec. Soc. **154**, G165 (2007).
[24] P.Repo, A. Haarahiltunen, L. Sainiemi, M. Yli-Koski, H. Talvitie, M. C. Schubert, and H. Savin, IEEE J. Photovolt. **3**, 90 (2012).
[25] M. Otto, M. Kroll, T. Käsebier, R. Salzer, A. Tünnermann, and Ralf B. Wehrspohn, Appl. Phys. Lett. **100**, 191603 (2012).
[26] M. Becker, U. Gösele, A. Hofmann, and S. Christiansen, J. Appl. Phys. **106**, 074515 (2007).
[27] D. E. Kane and R. M. Swanson, Proceedings of the 18th IEEE Photovoltaic Specialists Conference, Las Vegas, 1985 (IEEE, New York, 1985), pp. 578-583.
[28] A. Richter, S. W. Glunz, F. Werner, J. Schmidt, and A. Cuevas, Phys. Rev. B **86**, 165202 (2012).
[29] Sentaurus Synopsys. (2012). Synopsys TCAD, release G 2012.06. Available: http://www.synopsys.com.
[30] J. Schön, A. Abdollahinia, R. Müller, J. Benick, M. Hermle, W. Warta, and M. C. Schubert, To be published in Energy Procedia, Proceedings of the 3rd SiliconPV conference, Hamelin, Germany, 2013.
[31] F. D. Heinz, W. Warta, and M. C. Schubert, Energy Procedia **27**, 208 (2012).
[32] J. Benick, B. Hoex, G. Dingemans, W. M. M. Kessels, A. Richter, M. Hermle, and S. W. Glunz, Proceedings of the 24th European PV Solar Energy Conference and Exhibition, Hamburg, Germany, 2009, pp. 863 – 870.
[33] A. Richter, J. Benick, and M. Hermle, Journal of Photovoltaics **3**, 236 (2013).

Copyright line will be provided by the publisher